Nanoscale radiotherapy with hafnium oxide nanoparticles

Laurence Maggiorella*[1], Gilles Barouch[2], Corinne Devaux[1], Agnès Pottier[1], Eric Deutsch[3], Jean Bourhis[3], Elsa Borghi[1] & Laurent Levy[1]

[1]Nanobiotix, 60 rue de Wattignies, 75012, Paris, France
[2]CEA, DEN, Cadarache, F-13108 Saint-Paul-lez-Durance, France
[3]Laboratoire radiothérapie moléculaire, INSERM 1030, Institut Gustave Roussy Villejuif Labex, LERMIT, Université Paris-Sud, France
*Author for correspondence: laurence.maggiorella@nanobiotix.com

Aim: There is considerable interest in approaches that could improve the therapeutic window of radiotherapy. In this study, hafnium oxide nanoparticles were designed that concentrate in tumor cells to achieve intracellular high-energy dose deposit. **Materials & methods:** Conventional methods were used, implemented in different ways, to explore interactions of these high-atomic-number nanoparticles and ionizing radiation with biological systems. **Results:** Using the Monte Carlo simulation, these nanoparticles, when exposed to high-energy photons, were shown to demonstrate an approximately ninefold radiation dose enhancement compared with water. Importantly, the nanoparticles show satisfactory dispersion and persistence within the tumor and they form clusters in the cytoplasm of cancer cells. Marked antitumor activity is demonstrated in human cancer models. Safety is similar in treated and control animals as demonstrated by a broad program of toxicology evaluation. **Conclusion:** These findings, supported by good tolerance, provide the basis for developing this new type of nanoparticle as a promising anticancer approach in human patients.

Radiotherapy is the utilization of ionizing radiation in oncology. The principle of radiotherapy is related to the delivery of electromagnetic or particulate radiation that will interact with biological matter. Particles or waves will create ionization that releases electrons and subsequent free radicals traveling within a defined volume and generating energy deposition into this volume [1]. The effectiveness of radiotherapy in eradicating a tumor principally depends on the total dose of radiation administered. However, the tolerance of normal tissue surrounding the tumor definitively limits the dose. Therefore, to achieve the intended therapeutic benefit, local or locoregional side effects related to radiotherapy are controlled by precisely defining ballistics and also by fractionating the doses of delivered radiation. The index for estimating the dose of radiation that can treat a tumor effectively while staying within the safety range is known as the therapeutic window. The ultimate goal of radiotherapy is to increase radiation doses in tumors without increasing the doses in surrounding healthy tissues. Looking at past and current developments, this concept of broadening the therapeutic window is the primary goal of recently developed technologies such as the integration of imaging for 3D dosimetry and tumor motion tracking equipment, as well as strategies relative to beam focus and its intrinsic physical properties (carbon ions, protons). Furthermore, the addition of other types of approaches, such as radiosensitizers and radioprotectors, has been well explored [2–7].

Can nanoparticles broaden the therapeutic window of radiotherapy?

Radiation dose deposit within tissues is linked to their ability to absorb/interact with x-rays. This absorption depends on electron density (mainly water in the case of tissues) and the energy used. Introduction of material with higher electron density into the x-ray pathway can increase absorption as compared with water. Utilization of nanoparticles has a particular advantage as they are able to achieve a large dispersion within tumor tissue and closely interact with specific subcellular structures.

A number of computing tools or mathematical codes based on the Monte Carlo calculations are available to quantify radiation dose deposit in tissues. Utilization of high atomic number (Z) nanoparticles is of great interest in radiotherapy, as calculations have demonstrated promising enhancement of radiation dose deposit, although only in the low-energy range [8,9]. In this previous nanoparticle model simulation, the radiation dose enhancement achieved by nanoparticles is based on the concept of

Keywords
cancer ■ hafnium oxide ■ nanoparticles ■ nanotechnology ■ NBTXR3 ■ radiotherapy ■ therapy

Research Article
Future Oncology

Future Medicine part of fsg

homogeneous (isotropic) distribution of the high-electron-density element.

In this article, the authors report on NBTXR3 nanoparticles composed of hafnium oxide, and present the rationale for the design of this new type of high-*Z* nanoparticle as an innovative approach in anticancer treatment. To validate the concept, the Monte Carlo calculations are performed based on a 'local model' simulation, which quantify a high-local-energy deposit resulting from this new type of high-*Z* nanoparticle activated by a high-energy photon source. Of the utmost importance, NBTXR3 intratumoral (IT) bioavailability is shown, with dispersion of nanoparticles in the three dimensions and persistence within the tumor structure. Antitumor activity demonstrated marked advantage in terms of survival, tumor-specific growth delay and local control in both human mesenchymal and epithelial tumor models. Furthermore, unchanged crystal structure was demonstrated after long-term residence of NBTXR3 nanoparticles *in vivo* in different organs of rodents.

Materials & methods

Materials

The NBTXR3 product is intended for IT injection. NBTXR3 is a nonpyrogen, sterile, white aqueous dispersion of hafnium oxide nanoparticles coated with a biocompatible agent that provides the nanoparticles with a negative surface charge and ensures their stability in aqueous solution at pH values of between 6 and 8. NBTXR3 nanoparticle concentration in vials for injection is 64 g/l.

Specifically, the studies reported in the present article were performed with nanoparticles presenting a hydrodynamic diameter and a polydispersity index (which estimates the width of the distribution), determined by dynamic light scattering technique (Zetasizer NanoZS, Malvern Instruments Ltd, Malvern, UK), of approximately 50 nm and 0.100, respectively. The negative surface charge of the nanoparticles, as estimated by ζ-potential analysis (Zetasizer NanoZS), was approximately -50 mV. Spherical nanoparticle shape was determined using transmission electron microscopy technique (JEOL JEM 100CX operating at 100 kV, Service de Microscopie Electronique, UMR 7197, UPMC, Paris, France).

For clonogenic survival assay, NBTXR3 was diluted directly in growth media prior to treatment. For *in vivo* experiments, NBTXR3 was diluted prior to the injection with sterile glucose solution.

Irradiation conditions

Irradiations were delivered locally with a cobalt-60 source (average photon energy: 1.25 MeV, ALCYON, Institut Gustave Roussy, Villejuif, France) at a dose rate of 0.66 or 0.46 Gy/min, a 6-MV accelerator (SIRIUS, Institut Gustave Roussy) at a dose rate of 1 Gy/min or an applicator coupled to a curietherapy device containing a high-dose-rate iridium-192 source (average photon energy: 0.38 MeV).

Monte Carlo calculations

The performance (radiation dose enhancement) was explored by modeling the interaction of nanoparticles and the external x-ray beam, which was a monochromatic photon source of 200 KeV, 1 MeV or 6 MeV, considering the atomic number $Z_{\text{nanoparticle}}$ is equal to Z_{Hafnium}. Simulations (PENELOPE code calculation) of the generation of electrons and photons, and simulations of all subsequent generations of electrons and photons, were performed [10]. Two models were addressed:

- A 'global model' where a high-*Z* element is distributed homogeneously. Radiation dose enhancement (defined as dose deposition in the tumor with high-*Z* nanoparticles divided by dose deposition in the tumor without nanoparticles) results from energy deposition considering an averaged *Z* value (Z_{global}):

$$Z_{global} = (100 - x) \times Z_{water} + x \times Z_{nanoparticles} \quad (1)$$

  where x represents the concentration of nanoparticles within the tumor (mass of nanoparticles divided by the mass of the tumor). The nanoparticles increased the average efficacy of x-ray absorption in an isotropic fashion;

- A 'local model' where nanoparticles are clustered and high $Z_{\text{nanoparticles}}$ and Z_{water} are to be considered independently. In this simulation, a cube of 10 µm in size is filled with high-*Z* nanoparticles (composed of hafnium) and represents a nanoparticle cluster. The nanoparticle cluster is disposed within a cube of 100 µm in size filled with water, corresponding to a cell (water cell). The concentration of nanoparticles is equal to 0.1% (by volume) of any cell.

Cell lines & culture conditions

The HT1080 cell line, a human fibrosarcoma model (ATCC CCL-121), and the HCT 116

cell line, a human colorectal tumor cell line (ATCC CCL-247), were purchased at the American Type Culture Collection (MD, USA). The A673 cell line, a human Ewing family type sarcoma model, was purchased at the CLS Cell Lines Service (Eppelheim, Germany). HT1080 and A673 cells were grown in Dulbecco's Modified Eagle's Medium with GlutaMAX™ (Gibco®, Invitrogen, France). HCT 116 cells were grown in McCoy's 5a medium (Gibco). All cells were supplemented with 10% of inactivated fetal calf serum (Gibco) and 1% penicillin/streptomycin (Gibco) and maintained in an incubator at 37°C under 5% CO_2 humidified atmosphere.

Clonogenic survival assay

To test the survival of the HT1080 cell line, a clonogenic survival assay was performed [11]. Briefly, cells were plated in six-well plates within the range of 200–1000 cells per well. Once cells were attached to the plate, they were exposed to NBTXR3, radiation or both. The cells were irradiated 15–16 h post-NBTXR3 treatment with a single dose delivery (0 Gy [sham control], 1, 2, 3 or 4 Gy) using a cobalt-60 source or 6-MV accelerator. The cells were cultured for up to 10 days at 37°C under 5% CO_2 humidified atmosphere to allow them to form colonies. The colonies were fixed and stained with crystal violet solution (Sigma-Aldrich, MO, USA) and individual colonies were counted using the standard procedure [11].

In vivo assays

In vivo experiments were performed in animal care units authorized by the French ministries of Agriculture and Research and in accordance with European ethical guidelines of animal experimentation.

NBTXR3 IT bioavailability

Female SWISS nude mice aged 6–7 weeks were provided by the accredited breeder Charles River (L'Arbresle, France). HCT 116 xenografted tumors were obtained by subcutaneous (sc.) injection of 3×10^6 cells in the lower right flanks of the mice. One single IT injection of NBTXR3 was performed when the tumor volume reached 150 ± 30 mm^3. NBTXR3 presents a high contrast level and is easily visualized by x-ray microtomography. Microcomputerized tomography was used for evaluation of 3D dispersion and persistence of NBTXR3 within the tumor structure (eXplore Locus MicroCT system, GE Healthcare, Little Chalfont, UK). 3D reconstruction of MicroCT scan images and analysis were performed by VOXCAN (Marcy l'Etoile, France). The location of NBTXR3 nanoparticles at the cellular level was assessed using Zeiss EM 902 transmission electron microscope at 80 kV (C Longin; MIMA2; Plateau de Microscopie Electronique, Unité GPL, Jouy-en-Josas, France). Microphotographs were acquired using a MegaView III charge-coupled device camera and analyzed with ITEM software (Eloïse Sarl, Roissy CDG, France).

In vivo/*in vitro* clonogenic assays

Female nude NMRI mice aged 6–7 weeks were provided by the accredited breeder Janvier (CERT, Le Genest St Isle, France). HT1080 xenografted tumors were obtained by sc. injection of 3×10^6 cells in the lower right flanks of the mice. Mice were subjected to doses of 0, 4 and 8 Gy, using a cobalt-60 source, 24 h after IT injections of 5% glucose as vehicle or NBTXR3 product. Each mouse was sacrificed immediately after irradiation. HT1080 xenografted tumor was excised, mechanically minced with sterile scissor and scalpel and enzymatically digested in Accumax™ solution (Chemicon International, Millipore, Molsheim, France). After filtration, the single-cell suspension was seeded into 100-mm petri dishes within the range of 200–6000 cells per petri dish according to the treatment of NBTXR3 and irradiation doses. Clonogenic assays were performed as described elsewhere [11].

Terminal deoxynucleotide transferase-mediated dUTP nick end labeling staining

Apoptotic cells of tumor tissues were detected by measurement of nuclear DNA fragmentation using terminal deoxynucleotide transferase-mediated dUTP nick end labeling system (Roche Diagnostics, Basel, Switzerland), following the manufacturer's instruction.

In vivo antitumor effect in A673 mesenchymal tumor model

Female nude NMRI mice aged 6–7 weeks were provided by the accredited breeder Janvier. A673 xenografted tumors were obtained by sc. injection of 4×10^6 cells in the lower right flanks of the mice. Mice were irradiated by a single dose of 15 Gy using a cobalt-60 source, 24 h after IT injection of either 5% glucose as vehicle or NBTXR3 product. Mice were evaluated three-times per week, weighed and tumor volume was estimated from 2D tumor

measurements with a digital caliper using the formula

$$\frac{(l \times w^2)}{2} \quad (2)$$

where w = width and l = length in mm of the tumor. Treatment efficacy was determined using the following criteria: specific growth delay and the optimal growth inhibition (treated vs control groups [%]) according to Langdon *et al.* [12].

In vivo antitumor effect in HCT 116 epithelial tumor model

Female SWISS nude mice aged 6–7 weeks were provided by the accredited breeder Charles River. HCT 116 xenografted tumors were obtained by sc. injection of 3×10^6 cells in the lower right flanks of the mice. Two experiments were performed. In the first experiment the animals were irradiated or not by two sessions of 4 Gy using an iridium-192 source, 24 h and 48 h after IT injection of either 5% glucose as vehicle or NBTXR3 product. In the second experiment the animals were irradiated or not by a single session of 8 Gy using an iridium-192 source, 24 h after IT injection of either 5% glucose as vehicle or NBTXR3 product. Mice were evaluated twice per week, weighed and tumor volume was estimated as previously described.

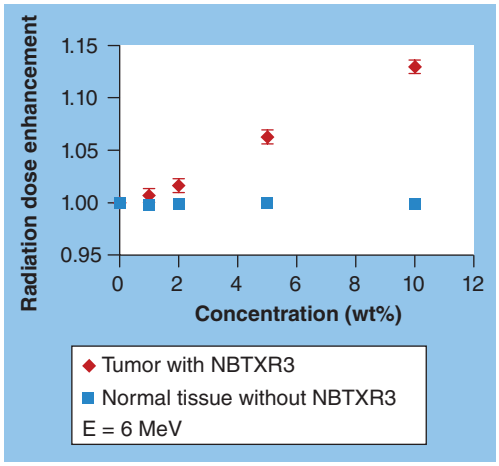

Figure 1. 'Global model' simulation.
The effect of nanoparticle concentration on radiation dose enhancement. Radiation dose enhancement calculation was performed using 'global model' simulation and a 6-MeV photon beam for both tumor with deep anatomical localization (with nanoparticles) and normal tissues (without nanoparticles). A Z_{global} is used for the calculation (Equation 1), where x represents the concentration of nanoparticles within the tumor (mass of nanoparticles divided by the mass of the tumor) and $Z_{nanoparticles}$ is equal to $Z_{hafnium}$.

Statistical analysis

Survival plots were generated using the Kaplan–Meier method, and differences between groups were determined by the Mantel–Cox test.

Results

High-*Z* nanoparticles follow the 'local model' Monte Carlo simulation

Modeling external beam radiotherapy interaction with high-Z nanoparticles (e.g., NBTXR3 or gold nanoparticles) using the 'global model' simulation may be considered a first approximation because it is far from reality. Figure 1 shows limited radiation dose enhancement in the 'global model' calculation for NBTXR3 nanoparticles activated by a 6-MeV monochromatic photon beam. Indeed, even if nanoparticles succeed in being well dispersed within the tumor, it was observed that nanoparticles present an anisotropic distribution at the cellular level. In fact, spatial disposition of nanoparticles can be considered as dots in a tumor and the Z may or may not be locally increased, depending on their presence or absence in a specific volume of the tumor structure. Figure 2 shows NBTXR3 nanoparticles clustered in vesicles (endosomes) in the cell's cytoplasm. The nanoparticles are present in the cell as dots forming clusters that determine an anisotropic absorption. Thus, the 'local model', where nanoparticles are clustered and high $Z_{nanoparticles}$ and Z_{water} are considered independently, corresponds to the real case (Figure 3A). Local dosimetry at the cellular level (within the water cell) demonstrated a higher localized radiation effect where there was presence of nanoparticles. Activation of these nanoparticles with high energy (1 or 6 MeV) demonstrated a local energy deposit within the volume occupied by the nanoparticles (Figure 3B). The calculated dose enhancement was approximately ninefold, taking the ratio of energy dose deposit of hafnium and water nanoparticles.

The two studies described in this article yielded evidence of increased deposit of energy in specific subcellular structures containing the nanoparticles (Figure 3C) via secondary electron emission (photoelectric and/or Compton effect), photon emission and also possibly via characteristic x-ray photon, Auger cascade and subsequent radical production. The energy release from these clusters of nanoparticles constitutes what we call a dose deposit 'hotspot', which could lead to high and localized destruction of biological subcellular structures and cell death.

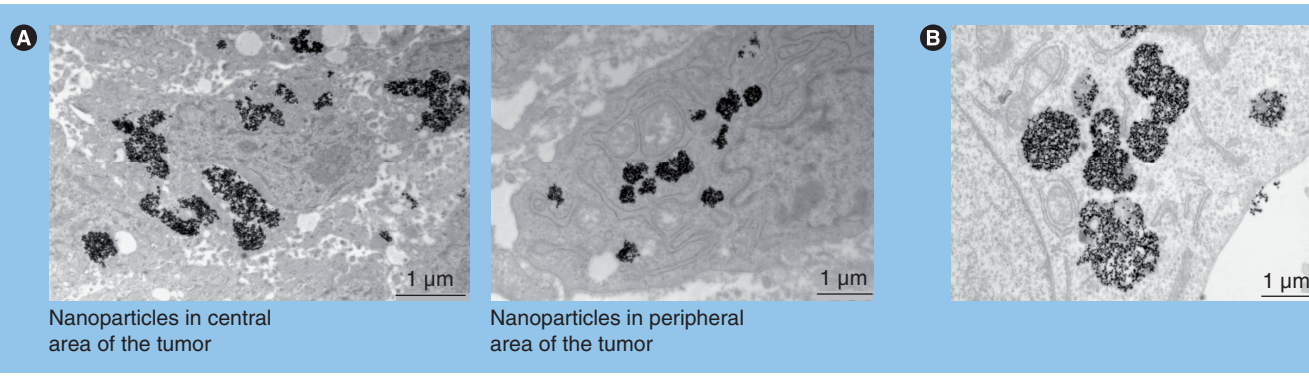

Figure 2. Anisotropic distribution of NBTXR3 nanoparticles at the cellular level. Nanoparticles are clustered in endosomes in the cell cytoplasm. **(A)** Typical transmission electron microscopy image of HCT 116 tumor (center and periphery of tumor). NBTXR3 nanoparticles were administered by intratumoral injection on HCT 116 tumor xenograft in nude mouse. Transmission electron microscopy images were performed 24 h after intratumoral injection. **(B)** Typical transmission electron microscopy image of cell (HT1080) following 12 h incubation with NBTXR3 nanoparticles (400 µM).

Dispersion of NBTXR3 nanoparticles within the tumor

NBTXR3 nanoparticles locally deposit a high level of energy when activated by ionizing radiation. Furthermore, several factors may contribute to achieve consistent tumor control, such as anatomic shape and the presence of nanoparticles with sufficient dispersion in three dimensions. Thus, studies assessed the locoregional localization of nanoparticles in terms of IT dispersion, potential leak and permanency within the 'gross tumor volume'. Figures 4A & 4B show good dispersion of NBTXR3 nanoparticles throughout the tumor volume following one IT injection. The nanoparticle dispersion appears both in central and peripheral areas of the tumor, within the tumor cells (Figure 2A).

Figure 4C shows the nanoparticle volume occupancy inside the tumor and the IT persistence of NBTXR3 over time. Microtomography was performed at 6 h, 1, 2, 7 and 14 days after one IT injection of NBTXR3 in HCT 116 tumor-grafted mice. The time of residency of nanoparticles in the tumor was demonstrated to be at least 14 days, and evaluation was no longer possible due to ethical mice sacrifice. It appears that the dispersion in the tumor remains equivalent over the tested period and that NBTXR3 'volume' image is not decreased over time, but rather there is a decrease of NBTXR3 volume/global tumor volume due to the rapid growth of the tumor. Few leakages of NBTXR3 from the tumor (less than 10%) were quantified by inductively coupled plasma mass spectrometry (data not shown). Nanoparticles' diffusion and amount within the tumor were also assessed using different schedules and NBTXR3 multi-injections (data not shown). Thus, for all the tested tumor models, volume and quantity of NBTXR3 were chosen based on microtomography observations showing optimum dispersion of NBTXR3 nanoparticles in three dimensions.

Local effect of nanoparticles activated with high energy in tumors

A 3D model is the only methodology that may demonstrate that dispersion of nanoparticles and their subcellular localization are crucial parameters for the enhancement of radiation-induced cell death response. The *in vivo*/*in vitro* clonogenic assay was selected as it is thought to be the best methodology to evaluate radio-enhancement (clonogenic capacity) *in vitro* when nanoparticles are previously exposed to the complexity of mammalian physiology. Activation of NBTXR3 nanoparticles using a cobalt-60 source led to a marked increase in the radiation response of HT1080 tumor xenografts with a mean dose enhancement factor (DEF) at 4 and 8 Gy above 1.5 (Figure 5A). In addition, no clonogenic toxicity of NBTXR3 nanoparticles injected in the HT1080 tumors was found (Figure 5B). Terminal deoxynucleotide transferase-mediated dUTP nick end labeling staining of histological tumor samples revealed an increase in the apoptotic response of cells treated with NBTXR3 nanoparticles and activated with irradiation in comparison with cobalt-60 irradiation alone (Figure 5C).

Radiation therapy based on the use of high-energy sources has proven a significant clinical benefit, including in survival. Thus, explorations with 'gold standard' clonogenic survival assays were performed using a cobalt-60 source and a 6-MV linear accelerator. Marked radio-enhancement was observed in the HT1080 fibrosarcoma cell line by activated NBTXR3 nanoparticles with irradiation (Figure 5D). Under both types of

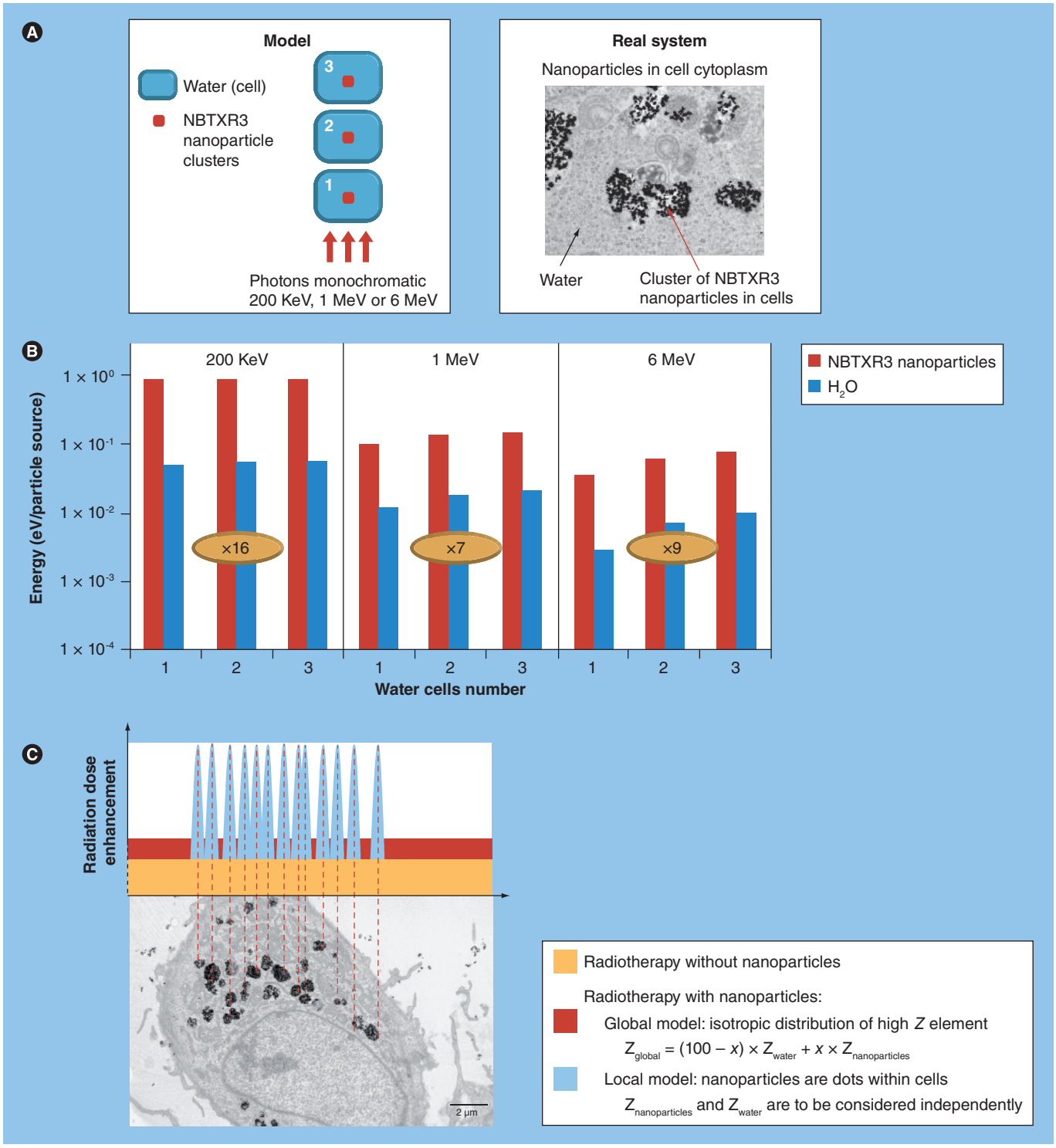

Figure 3. 'Local model' simulation. (A) 'Local model' simulation: a cube of 10 µm in size is filled with high-*Z* nanoparticles (composed of hafnium) and represents a nanoparticle cluster (red squares). The nanoparticle cluster is disposed within a cube of 100 µm in size filled with water (blue squares), corresponding to a cell. The concentration of nanoparticles is equal to 0.1% (by volume) of any cell. **(B)** Energy deposition using 'local model' simulation for monochromatic photon beam of 200 KeV, 1 MeV and 6 MeV: with nanoparticles (red); without nanoparticles (blue). **(C)** Radiation dose deposition is increased locally only where the NBTXR3 nanoparticles are (no enhancement effect in areas devoid of nanoparticles).

high-energy radiation, a significant decrease of the clonogenic surviving fraction was observed, and DEFs at 4 Gy were estimated at 1.4 ± 0.06 for 6 MV and 1.8 ± 0.09 for cobalt-60. As demonstrated by these two methodologies, activation of clusters of nanoparticles leads to marked

radio-induced cancer cell destruction. These findings confirm dose deposition 'hotspots' of radiation at the subcellular level, consistent with 'local model' calculation.

The antitumor activity of NBTXR3 was further evaluated in both mesenchymal and epithelial xenografted tumor models. The A673 Ewing's sarcoma model was chosen as reference sarcoma model engrafted in nude mice for NBTXR3 assessment. Refractory and/or recurrent Ewing's sarcoma remains a clinical challenge because the resistance of the disease to therapy makes it difficult to achieve durable results with standard treatments that include chemotherapy, radiation and surgery. Investigations to evaluate NBTXR3 antitumor effects on the A673 tumor model were performed using a high-energy cobalt-60 radiation source. Tolerance of the IT injection of NBTXR3 alone or activated by tumor γ-irradiation was estimated in comparison with control cohorts. No mouse death was observed over more than 50 days follow-up. No difference of toxicity was observed between animals treated with NBTXR3 (activated or not) and radiotherapy alone. The tumor regrowth delay (Figure 6A) demonstrated that the treatment schedule, one IT injection of NBTXR3 24 h prior to its activation, markedly increases the antitumor efficacy when compared with radiotherapy alone. An approximately twofold increase in tumor doubling time was observed associated with tumor growth inhibition of 82% for NBTXR3 activated by 15 Gy exposure, versus 72% for 15 Gy

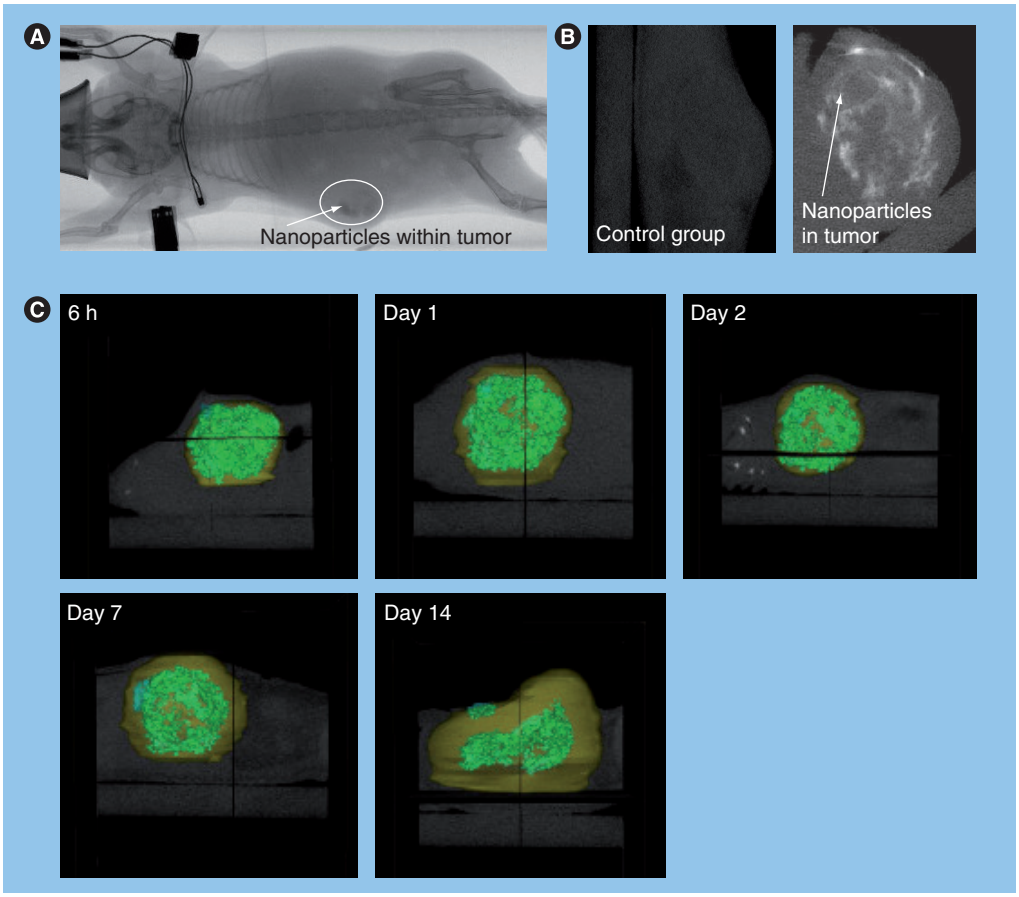

Figure 4. Spatial disposition of NBTXR3 nanoparticles. HCT 116 tumor xenograft in nude mouse. NBTXR3 nanoparticles were administered by intratumoral injection. Image acquisition was performed 24 h after intratumoral injection. **(A)** x-ray microtomograph image using SkyScan 1076 high-resolution *in vivo* scanner (acquisition performed by Animage, Bron, France; source: 50 kV; scan width: 35 mm; image pixel: 35.2 µm). **(B)** MicroCT scan images of the tumor without (control group) or with nanoparticles using the eXplore Locus MicroCT system (GE Healthcare, Little Chalfont, UK; acquisition performed by VOXCAN, Marcy l'Etoile, France; source: 80 kV and 450 µA; resolution acquisition: 45 µm). **(C)** NBTXR3 dispersion in three dimensions and persistence within tumor structure. 3D reconstruction slices 6 h, 1, 2, 7 and 14 days after one intratumoral injection of NBTXR3 in HCT 116 tumor xenograft. MicroCT scan images of the tumor with nanoparticles using the eXplore Locus MicroCT system (acquisition performed by VOXCAN; source: 80 kV and 450 µA; resolution acquisition: 45 µm). In green, NBTXR3 inside the tumor (yellow); in blue, NBTXR3 outside the tumor.

alone. Langdon's scoring of very active therapy was observed with NBTXR3 activated by 15 Gy exposure whereas 15 Gy showed moderate activity (Table 1) [12]. Kaplan–Meier curves associated with the tumor regrowth delay showed a significant increase (p = 0.0406) in the median survival time for NBTXR3 activated by 15 Gy exposure in comparison with 15 Gy alone, with 31 versus 25 days, respectively (data not shown).

Next, the HCT 116 tumor model, known as the radiosensitive model, was chosen as the reference epithelial tumor model for NBTXR3 assessment. As shown in Figure 6B, the tumor regrowth delay evaluation demonstrates that IT

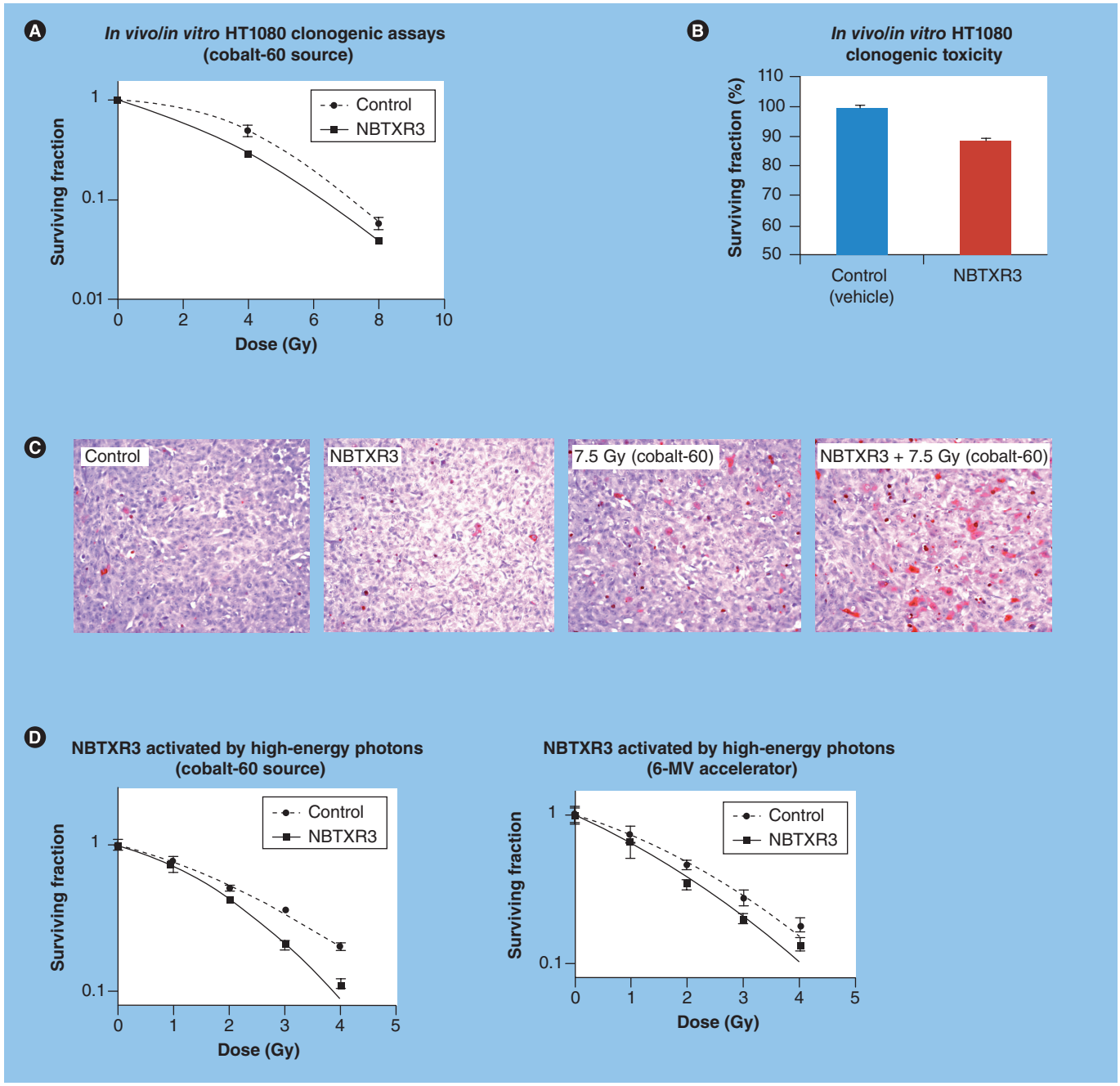

Figure 5. Local effect of NBTXR3 nanoparticles activated with high energy in tumor models. *In vivo*/*in vitro* clonogenic survival assays in HT1080 xenografted model in nude mouse. **(A)** NBTXR3 radioenhancement when activated with cobalt-60 irradiation. **(B)** No significant NBTXR3 clonogenic cytotoxicity after intratumoral injection in HT1080 tumor. Data are represented as the mean of surviving fraction ± standard error of the mean. **(C)** Terminal deoxynucleotide transferase-mediated dUTP nick end labeling staining of HT1080 tumors 24 h after activation of NBTXR3 by local irradiation with a cobalt-60 source. Terminal deoxynucleotide transferase-mediated dUTP nick end labeling apoptotic-positive cells are stained in red (magnification 200×). **(D)** NBTXR3 radioenhancement in human HT1080 fibrosarcoma cell line activated with high-energy ionizing radiation. HT1080 clonogenic survival assays of NBTXR3 activated with cobalt-60 source and with 6-MV accelerator. Data are represented as the mean of surviving fraction ± standard error of the mean.

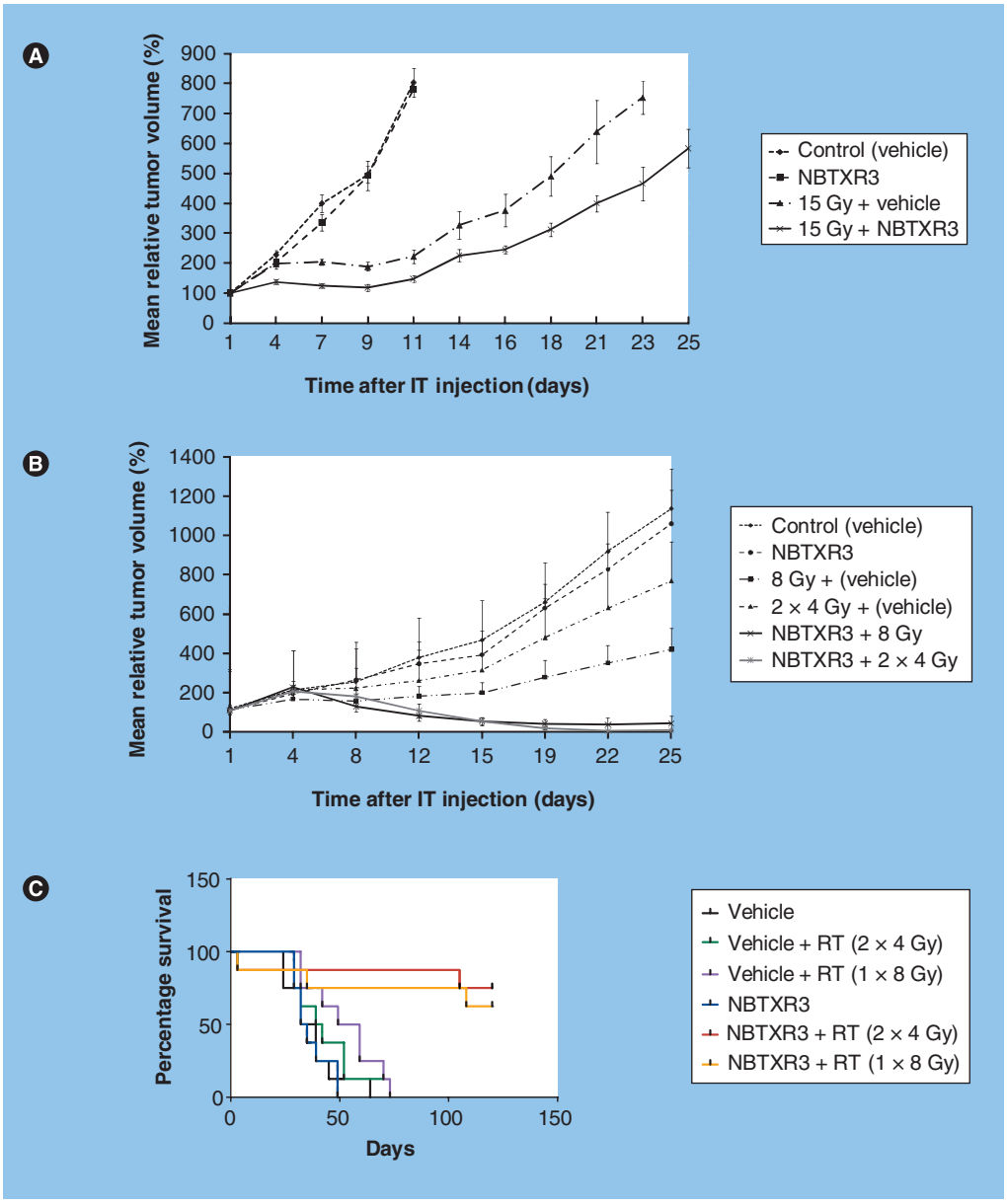

Figure 6. Antitumor activity of NBTXR3 activated by ionizing radiation in xenograft mouse models. (A) Tumor regrowth delay curves in A673 tumor model using high-energy cobalt-60 source. **(B)** Tumor regrowth delay curves and **(C)** Kaplan–Meier curves in HCT 116 tumor model using iridium-192 source.
IT: Intratumoral; RT: Radiotherapy.

injection of NBTXR3 24 h prior to its activation by either two doses of 4 Gy or one dose of 8 Gy using an iridium-192 energy source significantly increases the antitumor efficacy as compared with irradiation alone. Complete tumor response was observed in mice treated with NBTXR3 activated with 2 × 4 Gy and 8 Gy. Furthermore, the tolerance of IT injection of NBTXR3 not activated was equivalent across the studies. The Kaplan–Meier curves show significant difference ($p < 0.0100$) in overall survival of animals treated by NBTXR3 activated by either 2 × 4 Gy or 8 Gy at the cut-off date of 120 days (Figure 6C).

Overall, these data demonstrate that NBTXR3 produces a marked radioenhancement with very promising antitumor effects using high energy.

In vivo demonstration of unchanged crystal structure of NBTXR3

NBTXR3 nanoparticle design and subsequent rationale for development was based on the following:

Table 1. Level of antitumor activity of NBTXR3 according to Langdon's scoring in A673 tumor model using high-energy cobalt-60 source.

Vehicle	Optimal %T/C (days)	SGD	Efficacy scoring
NBTXR3	84 (7)	0.3	
15 Gy (vehicle)	28 (11)	1.3	(+)
15 Gy + NBTXR3	18 (11)	3.3	+++

SGD: Specific growth delay; T/C: Treated versus control groups.

- Physicochemical characterization of the nanomaterial;
- Metrics implementation in order to assess the nanoparticle's inherent features including chemical composition, crystal structure, mass, surface area, quantity evaluations and activation of a biological response to NBTXR3 nanoparticles;
- Knowledge about nanokinetics (biodistribution), including excretion after NBTXR3 intravenous injection.

Spatially (IT injection) and temporally (activation or nonactivation) controlled effects of injectable nanoparticles can lower the overall systemic dose and potential damage that these products would otherwise produce. Crystal integrity of the core of NBTXR3 nanoparticles over time after long storage in the body was demonstrated in animals after 6 months of exposure in the liver and spleen. This study was performed to detect structural changes of the hafnium oxide core and to determine potential crystal changes over time. NBTXR3 nanoparticles in aqueous suspension were used as baseline control material. Nanoparticle morphology, crystal structure and composition were evaluated by transmission electron microscopy, electron diffraction and microanalysis by energy dispersive spectroscopy (data not shown) on liver samples. The hafnium oxide nanoparticles did not undergo any change in terms of elemental composition and crystalline structure when compared with the baseline control nanomaterial.

Discussion

One of the primary research objectives in radiation therapy over the past decades has been the development of approaches that will enhance its effectiveness. Accurate delivery of the ionizing radiation dose has greatly improved, allowing more precise deposit of dose in the tumor while progressively reducing unwanted dose to surrounding healthy tissues. Despite such technical improvements, many patients still suffer from locally recurrent disease after radiotherapy and have significant toxicity.

This article presents the rationale for designing nanoparticles of hafnium oxide, to be activated by radiotherapy, which are capable of enlarging the therapeutic window by two prominent characteristics: their capacity of depositing high energy within tumors when the ionizing radiation source is 'on', and their chemically inert behavior in cellular and subcellular systems demonstrated by very good local and systemic tolerance, thus decreasing potential health hazards.

Conventional methods were used, although implemented in different ways, to explore interactions of high-*Z* matter and ionizing radiation with biological systems.

Nanoparticles: a new approach in the history of radiotherapy

Monte Carlo simulations using the 'global model' have been reported for gold nanoparticles with promising enhancement of radiation deposit using low-energy sources [8]. When this 'global model' concept is applied, the entire tumor has a greater absorption capacity (an average increase in electron density). Improvement in the model simulation was performed with calculations showing microscopic dose enhancement around gold nanoparticles under photon irradiation [13]. In parallel, several papers have been published on biological models showing the strong radioenhancement of gold nanoparticles, activated by radiotherapy, using photon energy sources in the kilovoltage range [14–19]. Liu *et al.* [16], Chithrani *et al.* [17] and Jain *et al.* [18] reported on clonogenic efficacy using gold nanoparticles activated by x-ray radiation operating at MV x-ray energies. Specifically, Chithrani *et al.* obtained a radiosensitization enhancement factor of 1.17 in HeLa cells treated with 50 nm-sized spherical gold nanoparticles and 6-MV energy photons. Jain *et al.* showed a radiation sensitizer enhancement ratio of 1.29 in MDA-MB-231 cells using spherical 1.9 nm-sized gold nanoparticles and 6-MV x-ray energies. These findings prove contradictory the prediction of the 'global model' with isotropic distribution of gold elements within the tumor.

In the present study, the Monte Carlo calculations and the importance of the 'local model' concept were biologically proven to be the relevant concept to evaluate radiation dose increase with high-*Z* nanoparticles activated by radiotherapy. In addition, the study of Kong

et al. suggested that localization of nanoparticles within the cells is an important factor in increasing radiation cytotoxicity [15]. Biological cellular systems determine distribution of nanoparticles in two areas: high concentration area and intracellular area without nanoparticles. Following the 'local model' simulation, high-local-energy deposit (increased approximately ninefold) surrounding the nanoparticles was observed by using high-energy monochromatic photon beams (1 and 6 MeV). Advantageously, NBTXR3 nanoparticles form clusters at the subcellular level that demonstrate their anisotropic dispersion in tumor models. NBTXR3 activated by a high-energy cobalt-60 source and 6-MV accelerator showed a marked DEF in a HT1080 fibrosarcoma tumor model. Indeed, no or very limited DEFs should have been observed at this high energy level according to the predictions of the 'global model'. The 'global model' underestimates the radiation dose enhancement and is thus not applicable to the authors' high-Z hafnium oxide nanoparticles.

Design of therapeutic nanoparticles

Undoubtedly, a deep understanding of how mammalian organ systems and their cells traffic their constituents to the correct location inside or outside the systems has supported hope to develop the most ambitious projects in nanomedicine. This knowledge permits the exploitation of cellular machineries for specific intracellular distribution and therapeutic availability, which, paralleled by a real insight into the chemistry, enlarges the field for rational design of nanoparticles for intracellular energy deposit.

Nanoparticle chemical composition is an essential characteristic controlling nanoparticle–ionizing radiation interactions. Nanoparticle characteristics (their size, shape and surface properties) will affect nanoparticle–biological component interactions. However, the potential toxicity of engineered nanomaterials developed for therapeutic application is to be considered, and encompasses phenomena such as release of toxic species into biological media, redox phenomena, electron transfer and reactive oxygen species (ROS) production. Also, adsorption of proteins on the nanoparticle surface may trigger various adverse phenomena such as changes in protein conformation and subsequent loss of enzyme activity, fibrillation or exposure to new antigenic epitopes.

Reviewing Mendeleev's periodic classification of elements allows one to realize that nanoparticles from metal cations in periods 4, 5, 6 and 7, including the lanthanides and actinides, are potential dose enhancers of radiation delivered to tissues.

Among metal nanoparticles (e.g., nanoparticles formed from the metal cations Au^{3+} and Pt^{2+}), gold nanoparticles (Z_{Au} = 79) are widely used for diagnosis and therapy [14–21]. However, in recent years, some publications have questioned the inert (i.e., absence of significant toxicity) behavior of synthesized gold nanoparticles in biological media [22–24]. Gold nanoparticles have a chemically active surface, and strong interactions between their surfaces and protein SH domains may occur, leading to protein conformation changes [25].

Metal oxide nanoparticles constitute an interesting alternative for medical use. Desired characteristics of metal oxide nanoparticles, such as size, shape and crystalline structure, are achieved using well-controlled chemistry in aqueous medium [26].

Chemical stability in biological media of engineered metal oxide nanoparticles is essential when one considers their potential toxicity: nanoparticles may be oxidized, reduced and dissolved, leading to a release of toxic ions [27].

Solubility of oxides of divalent elements increases in neutral and acidic aqueous solutions. Zinc oxide nanoparticles were reported to produce cellular toxicity triggered by zinc oxide dissolution and release of Zn^{2+} ions in body fluids and tissue/cellular media [25]. Regarding oxides of trivalent elements such as iron and aluminum, they were shown to adsorb natural organic materials and organic acids, which promote their dissolution.

NBTXR3 nanoparticles are composed of crystalline hafnium oxide. They have a very low solubility throughout a large pH range, which is inherent to oxide nanoparticles from metal cations with a +4 oxidation state.

Nanoparticle cellular toxicity includes generation of ROS. ROS form as a natural byproduct of the normal metabolism of oxygen and have important roles in cell signaling. However, during times of environmental stress (e.g., UV or heat exposure), ROS levels can increase dramatically and this can result in significant damage to cell structures. This culminates in a situation known as oxidative stress. In the case of cerium(IV) oxide nanoparticles, redox phenomena – Ce(IV)/Ce(III) cycle – at the cerium oxide surface have been described to induce oxidative stress and DNA damage *in vitro* [28]. The stable +4 oxidation state of hafnium is well known. Additionally, hafnium oxide is an electrical insulator with a band gap close to 6 eV [29].

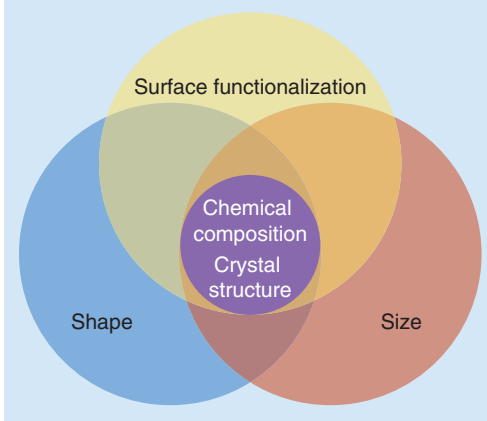

Figure 7. Design of therapeutic nanoparticles. Control of nanoparticles' main attributes: nanoparticle characteristics (chemical composition, crystal structure, size and shape) and nanoparticle surface functionalization.

Thus, hafnium oxide nanoparticles are unlikely to be involved in redox phenomena or electron transfer mechanisms in biological media.

Hafnium oxide particles in aqueous media in the presence of sodium perchlorate have been reported to have a point of zero charge of 7.4 [30]. The point of zero charge is defined as the pH of the medium for which the surface charge becomes zero. Thus, no marked surface acido-basicity is expected at neutral pH for hafnium oxide nanoparticles.

On the basis of hafnium oxide material properties, crystalline hafnium oxide nanoparticles were chosen for their promising benefit:risk ratio for human healthcare. Hafnium presents a high atomic number (Z = 72), which is crucial for efficient hafnium oxide nanoparticle–ionizing radiation interactions. Hafnium oxide nanoparticles are expected to have inert behavior in biological media, low solubility, absence of redox phenomena or electron transfer and no marked surface acido-basicity. In other words, their inert behavior, demonstrated in several biological systems (data not shown), has suggested the relevance of hafnium oxide selection.

Coating of nanoparticles with protective shells (surface functionalization) appears to be an effective means of preventing their dissolution and release of toxic ions. Surface functionalization may inhibit physicochemical mechanisms that can occur at the surface of inorganic nanoparticles (e.g., redox properties), which are responsible for nanoparticle toxicity. However, many coatings are labile and/or biodegradable in biological environments, and an initially nontoxic nanoparticle may ultimately display deleterious properties after shedding its shell. Furthermore, nonspecific coating (i.e., exclusion of specific biological molecular targets) may be an important factor in controlling nanoparticle–cell interactions and consequently nanoparticle efficacy. NBTXR3 nanoparticles are coated with a simple chemical envelope that provides them with a negative surface charge at neutral pH. NBTXR3 nanoparticle interaction with the cytoplasmic membrane is independent from specific processes of internalization [25,31].

Colloidal substances underlying no degradation (or poor degradation), such as gold and NBTXR3 nanoparticles, give rise to marked uptake by the mononuclear phagocytic cells (reticulo-endothelial system). 'Nanokinetics', or the concept of specific type and course of time of nanoparticles in the body, cannot be considered equivalent to the classical concept of monocompartmental/bicompartmental pharmacokinetics. However, nanokinetics is a determinant parameter of efficacy and safety prediction (i.e., expected side effects). Unlike small molecules, nanoparticle passage into tissues relies on the structure of endothelial fenestrae. These openings in the endothelial structure and their consequent density determine the bioavailability (passage of nanoparticles) into tumor and organ tissues. Nanoparticle shape and size are physical characteristics known to affect biological functions such as phagocytosis, body circulation and adhesion. For gold nanoparticles, Chithrani and colleagues showed that spherical 50 nm-sized gold nanoparticles coated with citrate molecules achieved the greatest cellular uptake compared with 14 or 74 nm-sized gold nanoparticles [32,33]. According to the authors, the spherical shape was found to be more effective for cell uptake compared with rod-shaped gold nanoparticles. Hafnium oxide nanoparticles (NBTXR3) are 50 nm-sized spheres. Consequently, NBTXR3 nanoparticle characteristics – size, shape and

Table 2. Key characteristics of NBTXR3 nanoparticles composed of crystalline hafnium oxide.

Characteristics	Relevance
Material composition/crystal structure: crystalline, hafnium oxide (HfO_2)	High-Z element (hafnium) for matter–energy interaction, inert behavior in biological media
Size: 50 nm	Biodistribution, EPR effect, reticuloendothelial system capture, excretion kinetics and pathway, barrier passage
Shape: spheres	Distribution, blood circulation, cell uptake
Surface charge: negative	Organ distribution, circulation time, cell membrane binding, cell uptake

EPR: Enhanced permeability and retention.

surface charge – are designed for efficient nanoparticle trafficking at the cellular level: cell membrane binding and cellular uptake. Figure 7 illustrates the nanoparticle's main attributes that are controlled during the manufacturing process. Table 2 summarizes the key characteristics of NBTXR3 nanoparticles.

Proof of concept of antitumor efficacy in animal models

Radioresistant and radiosensitive human tumor xenograft models from mesenchymal and epithelial cell lines were investigated for NBTXR3 tolerance and antitumor efficacy in activated state by different energies of ionizing radiation.

Several experiments evaluated the IT injection of NBTXR3 as well as nanoparticle dispersion, potential leak and permanency within the tumor volume. Very good benefit:risk ratio was observed in all explored tumors. Quantitative assessment of NBTXR3 by inductively coupled plasma mass spectrometry within tumor structure, surrounding skin and muscle at different time points, and concomitant dosage of NBTXR3 in plasma and organs, was performed to obtain more accurate information about the permanence of NBTXR3 within the tumor and its potential leak within the healthy surrounding tissues (data not shown). The experiments demonstrated low hafnium content in all organs when compared with the IT bioavailability.

Tolerance of the IT injection of NBTXR3 not activated or activated by ionizing radiation was evaluated in comparison with control cohorts in all *in vivo* xenograft models. No toxicity difference was observed between tested and control groups, suggesting absence of toxicity related to this treatment modality.

The antitumor effect of NBTXR3 activated by ionizing radiation was assessed in mesenchymal tumors (HT1080 human fibrosarcoma cell line and A673 human Ewing's sarcoma cell line) and epithelial tumors (HCT 116 human colon cancer cell line) xenografted in nude mice. Cobalt-60 activation of NBTXR3 leads to a major radioenhancement effect in *in vivo*/*in vitro* study. This methodology allows *in vivo* NBTXR3 activation by local irradiation of the tumor and *in vitro* exact quantification of radiation response of cells from the 3D tumor environment. Another radiation modality, brachytherapy (curietherapy) containing high-dose-rate iridium-192 sources, was also chosen to evaluate NBTXR3 antitumor effects in a HCT 116 radiosensitive tumor model. NBTXR3 showed marked advantage in terms of survival, tumor-specific growth delay and local control when compared with radiation therapy alone.

Executive summary

Design of therapeutic nanoparticles as a new approach to improve the therapeutic window of radiotherapy

- The rationale for designing nanoparticles made of hafnium oxide activated by radiotherapy is presented. The nanoparticles are capable of enlarging the therapeutic window owing to two prominent characteristics: their capacity to deposit high energy within tumors when the ionizing radiation source is 'on', and their chemically inert behavior in cellular and subcellular systems, demonstrated by very good local and systemic tolerance, thus decreasing potential health hazards.
- Using Monte Carlo simulation, activation of these nanoparticles with high-energy source (1 or 6 MeV) demonstrated a local energy deposit within the volume occupied by the nanoparticles with a calculated dose enhancement of approximately ninefold. In addition, the presence of NBTXR3 nanoparticles in the cell cytoplasm forming clusters was demonstrated in tumor cells.
- Crystalline hafnium oxide nanoparticles were chosen for their promising benefit:risk ratio for human healthcare. Hafnium presents a high atomic number of 72, which is crucial for efficient hafnium oxide nanoparticles–ionizing radiation interactions. Hafnium oxide has physicochemical properties that should not induce significant adverse effects. NBTXR3 nanoparticle characteristics – size, shape and surface charge – are designed for efficient cell membrane binding and cellular uptake of nanoparticles.
- *In vivo*/*in vitro* clonogenic assay and *in vitro* clonogenic survival assays in the HT1080 fibrosarcoma cell line by activated NBTXR3 nanoparticles with high-energy sources demonstrated marked radio-induced cancer cell destruction that confirms dose deposition 'hotspots' of radiation at the subcellular level, consistent with the 'local model' calculation.

Proof of concept of antitumor efficacy in animal models

- Antitumor activities demonstrated marked advantage in terms of survival, tumor-specific growth delay and local control in both mesenchymal and epithelial human tumor xenografted models using high-energy source, when compared with radiation therapy alone.
- No difference of local safety and tolerance was observed between tested and control groups.

Hafnium oxide crystal integrity

- Unchanged crystal structure of hafnium oxide was demonstrated after long-term residence *in vivo* in different organs of rodents.
- Very good safety and tolerance were observed in the nonclinical toxicology evaluation.

Clinical implications

- The data support the use of this new type of high-atomic-number nanoparticle as an innovative approach in anticancer therapy, with an on/off mode of action through successive fractions of radiation therapy using current radiotherapy equipment available in hospitals.

Taken together, these data provide the demonstration of the proof of concept of NBTXR3 nanoparticle antitumor performance. They provide the rationale and guidance for the clinical development of NBTXR3.

Hafnium oxide crystal integrity & clinical implications

For the first time, integrity of the hafnium oxide nanoparticle crystal structure was demonstrated in Kupffer's cells after chronic exposure in rodents. This is a remarkable property. Unchanged crystal structure of hafnium oxide is the key feature supporting the quality and the outcome of the interaction between these solid nanoparticles and ionizing radiation, allowing the on/off mode of action through successive fractions of radiation therapy.

In the meantime, specific immunology safety explorations suggest that NBTXR3 taken up by phagocytic cells does not have any significant toxicity on their viability. Local tolerance studies after exposure for 13 and 26 weeks showed no evidence of local intolerance and no irritant potential. Otherwise, NBTXR3 is not a mutagenic product (absence of genotoxicity), as demonstrated in *in vitro* and *in vivo* studies (data not shown).

Conclusion & future perspective

Changing the radiotherapy benefit:risk ratio is challenging. Despite of the development of multiple approaches, a significant improvement in the therapeutic window is yet to be found.

In this light, we designed NBTXR3, a crystalline hafnium oxide nanoparticle, activated by radiotherapy, capable of enlarging the therapeutic window both by high-energy deposit within the tumor tissue and its chemically inert behavior in cellular and subcellular systems, eliminating most of the potential health hazards. The data support the use of this new type of high-*Z* nanoparticle as an innovative approach in radiotherapy, with an on/off mode of action through successive fractions of radiation therapy using current radiotherapy equipment available in hospitals.

Financial & competing interests disclosure

L Maggiorella, C Devaux, A Pottier, E Borghi and L Levy are employees from Nanobiotix and have financial involvement with Nanobiotix, which is developing the NBTXR3 product discussed in the manuscript. C Devaux, A Pottier and L Levy are coinventors on a patent application related to NBTXR3 material. The authors have no other relevant affiliations or financial involvement with any organization or entity with a financial interest in or financial conflict with the subject matter or materials discussed in the manuscript.

No writing assistance was utilized in the production of this manuscript.

Ethical conduct of research

The authors state that they have obtained appropriate institutional review board approval or have followed the principles outlined in the Declaration of Helsinki for all human or animal experimental investigations.

References

Papers of special note have been highlighted as:
- ▪ of interest
- ▪▪ of considerable interest

1. Bernier J, Hall EJ, Giaccia A. Radiation oncology: a century of achievements. *Nat. Rev. Cancer* 4, 737–747 (2006).
2. Palma DA, Verbakel WF, Otto K, Senan S. New developments in arc radiation therapy: a review. *Cancer Treat. Rev.* 36, 393–399 (2010).
3. Martin A, Gaya A. Stereotactic body radiotherapy: a review. *Clin. Oncol.* 22, 157–172 (2010).
4. Matuszak MM, Di Y, Grills I, Martinez A. Clinical applications of volumetric modulated arc therapy. *Int. J. Radiat. Oncol. Biol. Phys.* 77, 608–616 (2010).
5. Amaldi U, Bonomi R, Braccini S *et al.* Accelerators for hadrontherapy: from Lawrence cyclotrons to linacs. *Nucl. Instrum. Methods Phys. Res. A* 620, 563–577 (2010).
6. Giro C, Berger B, Bölke E *et al.* High rate of severe radiation dermatitis during radiation therapy with concurrent cetuximab in head and neck cancer: results of a survey in EORTC institutes. *Radiother. Oncol.* 90, 166–171 (2009).
7. Schweitzer AD, Revskaya E, Chu P *et al.* Melanin-covered nanoparticles for protection of bone marrow during radiation therapy of cancer. *Int. J. Radiat. Oncol. Biol. Phys.* 78, 1494–1502 (2010).
8. Cho SH. Estimation of tumor dose enhancement due to gold nanoparticles during typical radiation treatments: a preliminary Monte Carlo study. *Phys. Med. Biol.* 50, N163–N173 (2005).

▪ **Monte Carlo calculation is used to estimate the radiation dose enhancement within a tumor when gold nanoparticles are accumulated in the tumor structure. In this calculation, the 'global model', where a high-atomic-number element (gold) is distributed homogeneously, is used.**

9. Roeske JC, Nunez L, Hoggarth M, Labay E, Weichselbaum RR. Characterization of the theorectical radiation dose enhancement from nanoparticles. *Technol. Cancer Res. Treat.* 6, 395–401 (2007).
10. Salvat F, Fernandez-Varea JM, Sempau J. *PENELOPE – A Code System for Monte Carlo Simulation of Electron and Photon Transport: Workshop Proceedings, Issy-les-Moulineaux, France, 7–10 July 2003.* Nuclear Energy Agency, Paris, France (2003).
11. Franken NA, Rodermond HM, Stap J, Haveman J, van Bree C. Clonogenic assay of cells *in vitro*. *Nat. Protoc.* 1, 2315–2319 (2006).
12. Langdon SP, Hendriks HR, Braakhuis BJM *et al.* Preclinical Phase II studies in human tumor xenografts: a European multicenter follow-up study. *Ann. Oncol.* 5, 412–422 (1994).

13. Jones BL, Krishnan S, Cho SH. Estimation of microscopic dose enhancement factor around gold nanoparticles by Monte Carlo calculations. *Med. Phys.* 37, 3809–3816 (2010).
14. Herold DM, Das IJ, Stobbe CC, Lyer RV, Chapman JD. Gold microspheres: a selective technique for producing biologically effective dose enhancement. *Int. J. Radiat. Biol.* 76, 1357–1364 (2000).
15. Kong T, Zeng J, Wang X *et al.* Enhancement of radiation cytotoxicity in breast-cancer cells by localized attachment of gold nanoparticles. *Small* 4, 1537–1543 (2008).
16. Liu CJ, Wang CH, Chen ST *et al.* Enhancement of cell radiation sensitivity by pegylated gold nanoparticles. *Phys. Med. Biol.* 55, 931–945 (2009).
17. Chithrani BD, Jelveh S, Jalali F *et al.* Gold nanoparticles as radiation sensitizers in cancer therapy. *Radiat. Res.* 173, 719–728 (2010).

▪▪ **Radiosensitization is observed in HeLa cells treated with gold nanoparticles and irradiated with a high-energy photon beam, using the clonogenic survival assay. Using 50-nm gold nanoparticles, the radiosensitization enhancement factor was 1.17 for 6-MV energy photons.**

18. Jain SJ, Coulter JA, Hounsell AR *et al.* Cell-specific radiosensitization by gold nanoparticles at megavoltage radiation energies. *Int. J. Radiat. Oncol. Biol. Phys*. 79, 531–539 (2011).

▪▪ **Radiosensitization in MDA-MB-231 cells at megavolt x-ray energies was demonstrated with gold nanoparticles. Typically, a radiation sensitizer enhancement ratio of 1.29 was achieved using 6-MV x-ray energies and 1.9-nm gold nanoparticles.**

19. Hainfeld JF, Slatkin DN, Smilowitz HM. The use of gold nanoparticles to enhance radiotherapy in mice. *Phys. Med. Biol.* 49, N309–N315 (2004).

▪ **Presents the first *in vivo* study showing a marked antitumor efficacy using gold nanoparticles activated by x-rays when compared with radiation therapy alone. In this study, the photon energy source used was in the kilovoltage range.**

20. Hainfeld JF, Slatkin DN, Focella TM, Smilowitz HM. Gold nanoparticles: a new x-ray contrast agent. *Br. J. Radiol.* 79, 248–253 (2006).
21. Von Maltzahn G, Park JH, Agrawal A *et al.* Computationally guided photothermal tumor therapy using long-circulating gold nanorod antennas. *Cancer Res.* 69, 3892–3900 (2009).
22. Chen YS, Hung YC, Liau I, Huang GS. Assessment of the *in vivo* toxicity of gold nanoparticles. *Nanoscale Res. Lett.* 4, 858–864 (2009).
23. Sadauskas E, Danscher G, Toltenberg M, Vogel U, Larsen A, Wallin H. Protracted elimination of gold nanoparticles from mouse liver. *Nanomedicine* 5, 162–169 (2009).
24. Cho WS, Cho M, Jeong J *et al.* Acute toxicity and pharmacokinetics of 13 nm-sized PEG-coated gold nanoparticles. *Toxicol. Appl. Pharmacol.* 236, 16–24 (2009).
25. Nel AE, Mädler L, Velegol D *et al.* Understanding biophysicochemical interactions at the nano-bio interface. *Nat. Mater.* 8, 543–557 (2009).
26. Jolivet JP, Cassaignon S, Chanéac C, Chiche D, Durupthy O, Portehault D. Design of metal oxide nanoparticles: control of size, shape, crystalline structure and functionalization by aqueous chemistry. *C. R. Chim.* 13, 40–51 (2010).
27. Auffan M, Rose J, Wiesner MR, Bottero JY. Chemical stability of metallic nanoparticles: a parameter controlling their potential cellular toxicity *in vitro*. *Environ. Pollut.* 157, 1127–1133 (2009).
28. Auffan M, Rose J, Orsiere T *et al.* CeO_2 nanoparticles induce DNA damage towards human dermal fibroblasts *in vitro*. *Nanotoxicology* 3, 161–171 (2009).
29. Garcia JC, Lino AT, Scolfaro LM *et al.* First principles studies of relativistic and spin-orbit effects on the HfO_2 band structures. *Phys. Stat. Sol.* 1(Suppl. 1), S236–S240 (2004).
30. Kosmulski M. Attempt to determine pristine points of zero charge of Nb_2O_5, Ta_2O_5, and HfO_2. *Langmuir* 13, 6315–6320 (1997).
31. Wilhem C, Gazeau F. Universal cell labeling with ionic magnetic nanoparticles. *Biomaterials* 29, 3161–3174 (2008).
32. Chithrani BD, Ghazani AA, Chan WC. Determining the size and shape dependence of gold nanoparticle uptake into mammalian cells. *Nano Lett.* 6, 662–668 (2006).
33. Chithrani BD, Chan WC. Elucidating the mechanism of cellular uptake and removal of protein-coated gold nanoparticles of different sizes and shapes. *Nano Lett.* 7, 1542–1550 (2007).